Inorg. Chem. **2003**, *42*, 8270–8277

Transient Absorption Studies of the Pacman Effect in Spring-Loaded Diiron(III) μ-Oxo Bisporphyrins

Justin M. Hodgkiss, Christopher J. Chang, Bradford J. Pistorio, and Daniel G. Nocera*

Department of Chemistry, 6-335, Massachusetts Institute of Technology, 77 Massachusetts Avenue, Cambridge, Massachusetts 02139-4307

Received July 1, 2003

Picosecond transient absorption spectroscopy of diiron(III) μ-oxo bisporphyrins appended to xanthene, (DPX)Fe_2O and (DPXM)Fe_2O, and dibenzofuran (DPD)Fe_2O have been investigated in order to decipher the effect of a spring-loaded cleft on their photophysics and attendant oxidation photocatalysis. The tension of the cofacial pocket is systematically tuned with the bridge span and meso-substitution opposite to the bridge; the distances of the relaxed cofacial pockets and clamped Fe–O–Fe pockets are known from X-ray crystallography (Δd_{M-M}(relaxed − clamped) = 4.271 Å (DPD), 2.424 Å (DPXM), 0.208 Å (DPX)). The photophysical and chemical properties of these cofacial platforms are compared to the unbridged diiron(III) μ-oxo analogue, $(Etio)_2Fe_2O$. Photon absorption by the diiron(III) μ-oxo chromophore prompts Fe–O–Fe photocleavage to release the spring and present a $PFe^{IV}O/PFe^{II}$ pair (P = porphyrin subunit); net photooxidation is observed when oxygen atom transfer to substrate occurs before the spring can reclamp to form the μ-oxo species. The inherent lifetimes of the $PFe^{IV}O/PFe^{II}$ pairs for the four compounds are surprisingly similar (τ[(DPD)Fe_2O] = 1.36(3) ns, τ[(DPX)Fe_2O] = 1.26(5) ns, τ[(DPXM)Fe_2O] = 1.27(9) ns, and τ[$(Etio)_2Fe_2O$] = 0.97(3) ns), considering the structural differences arising from tensely clamped (DPD and DPXM), relaxed (DPX), and unbridged (Etio) cofacial architectures. However, the rates of net oxygen atom transfer for (DPD)Fe_2O and $(Etio)_2Fe_2O$ are found to be 4 orders of magnitude greater than that of (DPX)Fe_2O and 2 orders of magnitude greater than that of (DPXM)Fe_2O. These results show that the spring action of the cleft, known as the Pacman effect, does little to impede reclamping to form the μ-oxo species but rather is manifest to opening the cofacial cleft to allow substrate access to the photogenerated oxidant. Consistent with this finding, photooxidation efficiencies decrease as the steric demand of substrates increase.

Introduction

Single-electron transfer provides an efficient nonradiative channel by which molecules decay from their electronic excited states. For this reason, photoredox reactions of transition metal complexes involving more than one electron are unusual. One approach to achieving multielectron photoreactivity is predicated on the chemistry of two-electron mixed-valence excited states. These novel excited states may be prepared by exciting the metal-to-metal charge-transfer states arising from weakly coupled orbitals;[1−4] alternatively, the two-electron mixed-valence character may be conferred on the bimetallic core by appropriate ligand systems.[5−7] As one-electron mixed-valence complexes promote single-electron transfer reactions, a two-electron mixed-valence complex can promote reactions in two-electron steps at the individual metal centers of the bimetallic core.[5,8,9]

The photoinduced transfer of an atom not involving halogen or hydrogen offers another strategy to develop multielectron photochemistry. In the case of oxygen, a net redox change of two accompanies atom transfer. Oxygen atom transfer (OAT) continues to be a target of mechanistic inves-

* Author to whom correspondence should be addressed. E-mail: nocera@mit.edu.

(1) Engebretson, D. S.; Zaleski, J. M.; Leroi, G. E.; Nocera, D. G. *Science* **1994**, *265*, 759−762.
(2) Engebretson, D. S.; Graj, E.; Leroi, G. E.; Nocera, D. G. *J. Am. Chem. Soc.* **1999**, *121*, 868−869.
(3) Pistorio, B. J.; Nocera, D. G. *Chem. Commun.* **1999**, 1831−1832.
(4) Cotton, F. A.; Nocera, D. G. *Acc. Chem. Res.* **2000**, *33*, 483−490.
(5) Heyduk, A. F.; Macintosh, A. M.; Nocera, D. G. *J. Am. Chem. Soc.* **1999**, *121*, 5023−5032.
(6) Heyduk, A. F.; Nocera, D. G. *Chem. Commun.* **1999**, 1519−1520.
(7) Heyduk, A. F.; Nocera, D. G. *J. Am. Chem. Soc.* **2000**, *122*, 9415−9426.
(8) Odom, A. L.; Heyduk, A. F.; Nocera, D. G. *Inorg. Chim. Acta* **2000**, *297*, 330−337.
(9) Heyduk, A. F.; Nocera, D. G. *Science* **2001**, *293*, 1639−1641.

10.1021/ic034751o CCC: $25.00
Published on Web 11/11/2003

Chart 1

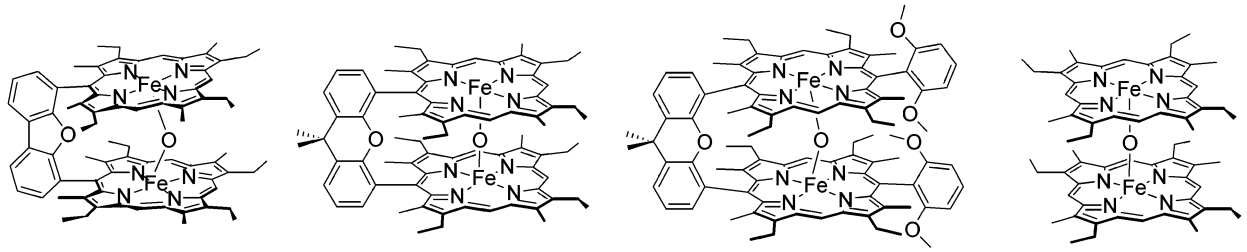

(DPD)Fe_2O (DPX)Fe_2O (DPXM)Fe_2O (Etio)$_2Fe_2O$

tigations,[10−13] owing to its significance in biological transformations,[14−16] prominence in organic[17−19] and inorganic[20,21] syntheses, and oxidation catalysis. These studies show that the oxygen transfer is preferred for the side-on approach of substrate to terminal metal−oxygen bonds. With this principle of OAT reactivity firmly established, we sought to develop photoactive metal platforms possessing architectures that would sterically constrain substrate attack to the electronically favored side-on geometry. Iron porphyrins were chosen as the metal−oxo platforms because these systems are known to utilize O_2 for oxidation reactions without the need for an external coreductant.[22−28] The general cycle utilizes a photon to cleave the thermally inert Fe−O bond of diiron(III) μ-oxo bisporphyrin to produce a terminal iron(IV) oxo, which is capable of oxygenating substrate with the concomitant formation of 2 equiv of reduced iron(II) porphyrin. Reaction of the two separate ferrous porphyrin subunits with O_2 re-forms the diiron(III) μ-oxo complex for re-entry into a catalytic cycle. The net OAT reaction of iron(IV) oxo porphyrins (compound II-type reactivity) is thought to proceed by electron transfer, mechanistically distinct from an authentic oxygen transfer of iron(V) oxo porphyrin cation radicals (compound I-type reactivity). In either case, however, the rate-limiting step involves attack of the ferryl oxygen on the substrate,[29] which can best access the d(Fe)−p(O) π^* orbital by a side-on approach. For the case of simple monomeric porphyrins, the reaction coordinate for substrate attack is ostensibly undirected. However, we have shown recently that the preferred side-on approach of substrate may be achieved when a single, rigid spacer juxtaposes the two cofacial porphyrins. In our design of these so-called Pacman porphyrins, the cofacial bisporphyrin bearing a dibenzofuran (DPD) spacer exhibits exceptional vertical flexibility.[30−32] Whereas the metal−metal distance of the diiron(III) μ-oxo (DPD)Fe_2O complex is 3.5 Å, the metal−metal distance of the relaxed DPD pocket is >7.5 Å.[30,31] This vertical flexibility of the DPD cleft is manifested in efficient OAT photochemistry. A comparative photochemical study of the spring-loaded (DPD)Fe_2O and non-spring-loaded (DPX)Fe_2O (DPX = xanthene spacer, relaxed DPX pocket 3.7 Å[30,33]) Pacman porphyrins has revealed a superior photoreactivity (ca. 10 000-fold) of the former.[30,34] This result suggests that the "molecular spring" action of the DPD scaffold can (i) hinder the regeneration of the diiron(III) μ-oxo precatalyst and/or (ii) more ably present the terminal metal oxo species for side-on attack by substrate. In an effort to distinguish between these two factors, we have undertaken time-resolved absorption studies of the molecular spring action of diiron(III) μ-oxo Pacman porphyrins with cofacial clefts of varying tension. The tension of the cofacial pocket is systematically tuned with the bridge span (DPX vs DPD) and meso-substitution of 2,6-dimethoxyaryl groups opposite to a DPX bridge; the distances of the relaxed cofacial pockets and clamped Fe−O−Fe pockets are known

(10) Veige, A. S.; Slaughter, L. M.; Wolczanski, P. T.; Matsunage, N.; Decker, S. A.; Cundari, T. R. *J. Am. Chem. Soc.* **2001**, *123*, 6419−6420.
(11) Veige, A. S.; Slaughter, L. M.; Lobkovsky, E. B.; Wolczanski, P. T.; Matsunaga, N.; Decker, S. A.; Cundari, T. R. *Inorg. Chem.* **2003**, *42*, 6204−6224.
(12) Crevier, T. J.; Mayer, J. M. *J. Am. Chem. Soc.* **1997**, *119*, 8485−8491.
(13) Hall, K. A.; Mayer, J. M. *J. Am. Chem. Soc.* **1992**, *114*, 10402−10411.
(14) Meunier, B.; Robert, A.; Pratviel, G.; Bernadou, J. In *The Porphyrin Handbook*; Kadish, K. M., Smith, K. M., Guilard, R., Eds.; Academic Press: San Diego, CA, 2000; Vol. 4, pp 119−187.
(15) Meunier, B. *Biomimetic Oxidations Catalyzed by Transition Metal Complexes*; Imperial College Press: London, 2000.
(16) Ortiz de Montellano, P. R. *Cyctochrome P450: Structure, Mechanism, and Biochemistry*, 2nd ed.; Plenum: New York, 1995.
(17) Jacobsen, E. N. *Acc. Chem. Res.* **2000**, *33*, 421−431.
(18) Kolb, H. C.; VanNieuwenhze, M. S.; Sharpless, K. B. *Chem. Rev.* **1994**, *94*, 2483−2547.
(19) Corey, E. J.; Noe, M. C. *J. Am. Chem. Soc.* **1996**, *118*, 11038−11053.
(20) Holm, R. H. *Chem. Rev.* **1987**, *87*, 1401−1449.
(21) Odom, A. L.; Cummins, C. C.; Prostasiewicz, J. D. *J. Am. Chem. Soc.* **1995**, *117*, 6613−6614.
(22) Ercolani, C.; Gardini, M.; Pennesi, G.; Rossi, G. *Chem. Commun.* **1983**, *10*, 549−550.
(23) Weber, L.; Haufe, G.; Rehorek, D.; Hennig, H. *Chem. Commun.* **1991**, *107*, 502−503.
(24) Weber, L.; Hommel, R.; Behling, J.; Haufe, G.; Hennig, H. *J. Am. Chem. Soc.* **1994**, *116*, 2400−2408.
(25) Hennig, H.; Luppa, D. J. *J. Prakt. Chem. (Weinheim, Ger.)* **1999**, *341*, 757−767.
(26) Peterson, M. W.; Richman, R. M. *J. Am. Chem. Soc.* **1982**, *104*, 5795−5796.
(27) Peterson, M. W.; Rivers, D. S.; Richman, R. M. *J. Am. Chem. Soc.* **1985**, *107*, 2907−2915.
(28) Peterson, M. W.; Richman, R. M. *Inorg. Chem.* **1985**, *24*, 722−725.
(29) Groves, J. T.; Gross, Z.; Stern, M. K. *Inorg. Chem.* **1994**, *33*, 5065−5072.
(30) Chang, C. J.; Baker, E. A.; Pistorio, B. J.; Deng, Y.; Loh, Z.-H.; Miller, S. E.; Carpenter, S. D.; Nocera, D. G. *Inorg. Chem.* **2002**, *41*, 3102−3109.
(31) Deng, Y.; Chang, C. J.; Nocera, D. G. *J. Am. Chem. Soc.* **2000**, *122*, 410−411.
(32) Chang, C. J.; Deng, Y.; Shi, C.; Chang, C. K.; Anson, F. C.; Nocera, D. G. *Chem. Commun.* **2000**, 1355−1356.
(33) Chang, C. J.; Deng, Y.; Heyduk, A. F.; Chang, C. K.; Nocera, D. G. *Inorg. Chem.* **2000**, *39*, 959−966.
(34) Pistorio, B. J.; Chang, C. J.; Nocera, D. G. *J. Am. Chem. Soc.* **2002**, *124*, 7884−7885.

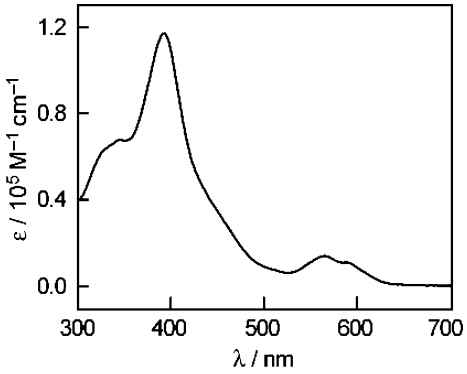

Figure 1. Electronic absorption spectrum of (DPD)Fe_2O in dry benzene.

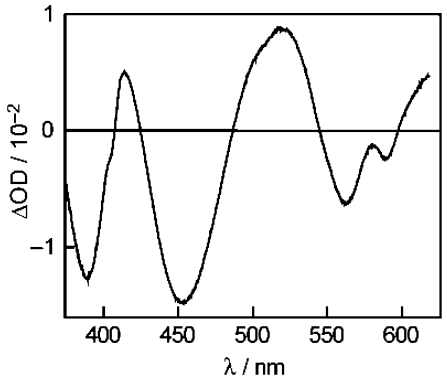

Figure 2. Transient absorption spectrum of (DPD)Fe_2O at 20 ps after the 100-fs, 405-nm excitation pulse.

from X-ray crystallography (Δd_{M-M}(relaxed − clamped) = 4.271 Å (DPD), 2.424 Å (DPXM), 0.208 Å (DPX)). The picosecond time-resolved kinetics of the cofacial complexes (DPD)Fe_2O, (DPXM)Fe_2O, and (DPX)Fe_2O have been measured and compared to the photophysical behavior of the unbridged analogue diiron(III) bisetioporphyrin (Etio) I, $(Etio)_2Fe_2O$ (Chart 1). Our findings reveal that the remarkably enhanced efficiency for photoinduced OAT of "spring-loaded" Pacman porphyrins is a direct consequence of the unique ability of the platform to undergo large, facile changes in vertical cleft size. Transient kinetics measurements show that the "spring" action of the DPD and DPXM platforms does little to impede reclamping of the Pacman cleft about the oxo intermediate. Rather, the spring action of the Pacman cleft provides access of substrate to the photogenerated terminal metal−oxo intermediate. Steady-state photochemical measurements of the efficiency of OAT as a function of the steric demands of the substrate are consistent with the results of transient kinetics measurements. Namely, the overall efficiency for the photoinduced OAT decreases as the steric bulk of the substrate increases. These results show that Pacman porphyrins afford a unique combination of synthetic availability and vertical flexibility and that these attributes may be effectively exploited in the design of multielectron atom transfer photocatalysts.

Results

Figure 1 shows an electronic absorption spectrum of (DPD)Fe_2O, which is essentially identical to that obtained for (DPX)Fe_2O, (DPXM)Fe_2O, and $(Etio)_2Fe_2O$. Four prominent absorption features dominate the spectrum with three corresponding to the characteristic absorptions of the porphyrin macrocycle: a Soret band appears at 395 nm and Q-bands appear at 565 and 590 nm. The absorption of particular relevance to this study is the ligand-to-metal charge-transfer (LMCT) absorption at 360 nm, which has unambiguously been assigned from a study of the halide dependence of the absorption energy maximum of the (TPP)Fe(X) series.[35] For the porphyrins that are the subject of this study, the LMCT parentage is the μ-oxo ligand. Consistent with this assignment, the action spectrum for OAT of photocatalysis for this series of diiron μ-oxo bisporphyrins tracks the LMCT absorption and not that of the Soret or Q-bands.[36] The assignment is further supported by the observation that the 360-nm absorption is absent from spectra of the stoichiometric photochemical reaction, in which the oxygen atom is removed from the porphyrin cleft by substrate.[30,34]

Figure 2 shows a transient absorption (TA) spectrum of (DPD)Fe_2O, 20 ps after excitation into the LMCT band. The spectra for (DPX)Fe_2O, (DPXM)Fe_2O, and $(Etio)_2Fe_2O$ match Figure 2, indicating that the intermediate formed is independent of the presence or nature of the bridge. Transient bleaches in the Q-band region (λ_{max} = 565 and 590 nm) as well as in the Soret band region (λ_{max} = 455 nm) are complemented by transient absorptions at 415 and 525 nm. The spectrum is consistent with the results obtained by Rentzepis' study of $(TPP)_2Fe_2O$ (TPP = tetraphenylporphyrin).[37] The observed spectrum is attributed to a single transient species because (i) nanosecond (ns) transient absorption spectroscopy shows no evidence of transient species on longer time scales (10−250 ns) and (ii) the transient signal returns to a $\Delta OD = 0$ with a monoexponential decay (vide infra) within ~5 ns of the excitation pulse.

The nature of the transient species is consistent with a photoproduct of LMCT excitation. It occurs on too long of a time scale to be associated with dynamics such as intramolecular or intermolecular (solvent-coupled) vibrational cooling (τ < 1 ps[38−42]), iron porphyrin excited-state decay (τ < 6 ps[43]), or bond cleavage resulting from LMCT excitation (τ < 1 ps[37,38]). Two chemically feasible photoproducts resulting from LMCT excitation are shown in Scheme 1. A dissociated $PFe^{II}/PFe^{IV}O$ pair prevails for the photoactivation of unbridged diiron(III) μ-oxo bisporphy-

(35) Hendrickson, D. N.; Kinnaird, M. G.; Suslick, K. S. *J. Am. Chem. Soc.* **1987**, *109*, 1243−1244.
(36) Pistorio, B. J. Ph.D. Thesis, Massachusetts Institute of Technology, 2003.
(37) Guest, C. R.; Straub, K. D.; Hutchinson, J. A.; Rentzepis, P. M. *J. Am. Chem. Soc.* **1988**, *110*, 5276−5280.
(38) Wang, W.; Ye, X.; Demidov, A. A.; Rosca, F.; Sjodin, T.; Cao, W.-X.; Sheeran, M.; Champion, P. M. *J. Phys. Chem. B* **2000**, *104*, 10789−10801.
(39) Rodriguez, J.; Kirmaier, C.; Holten, D. *J. Am. Chem. Soc.* **1989**, *111*, 6500−6506.
(40) Rodriguez, J.; Holten, D. *J. Chem. Phys.* **1989**, *91*, 3525−3531.
(41) Baskin, J. S.; Yu, H.-Z.; Zewail, A. H. *J. Phys. Chem. A* **2002**, *106*, 9837−9844.
(42) Yu, H.-Z.; Baskin, J. S.; Zewail, A. H. *J. Phys. Chem. A* **2002**, *106*, 9845−9854.
(43) Huppert, D.; Straub, K. D.; Rentzepis, P. M. *Proc. Natl. Acad. Sci. U.S.A.* **1977**, *74*, 4139−4143.

Scheme 1

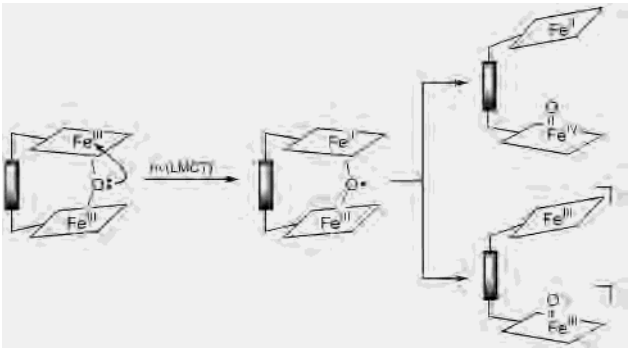

rins.[24,27,44] Transient Raman studies of photoexcited $(TPP)_2Fe_2O$ show a pronounced stretching vibration at 852 cm^{-1} in the resonance Raman spectrum. Isotope labeling experiments of independently prepared $(TPP)Fe^{IV}{=}O$ confirm the assignment of this signature band to $\nu(Fe^{IV}{=}O)$. No band is assigned to a $\nu(Fe^{III}{-}O^{-})$ stretching vibration, which is expected to occur at ~600 cm^{-1} based on a force constant of 3.80 mdyn/Å for an Fe−O single bond (as compared with 5.32 mdyn/Å[45] for the double bonded $PFe^{IV}{=}O$ species).[45−49] These photochemical results of unbridged porphyrins appear to hold for Pacman diiron(III) μ-oxo bisporphyrins. Namely, a $PFe^{II}/PFe^{IV}O$ pair is the predominant product of photoexcitation, based on the following observations. First, the transient absorption spectra of Pacman and unbridged diiron(III) μ-oxo bisporphyrins are identical. Second, the transient difference spectrum in Figure 2 is consistent with the production of a $PFe^{II}/PFe^{IV}O$ pair based on absorption spectra of model compounds. Finally, photoexcited Pacman compounds are competent oxidants of triphenyl- and alkylphosphines, dialkyl sulfides, and cycloalkenes;[30,34] in all cases, the oxidation reactivity of these substrates is known to be promoted by a ferryl species.[24,50,51] We therefore conclude that the transient intermediate responsible for the signal in Figure 2 is the "sprung open" Pacman composed of ferryl and ferrous subunits.

The kinetics for opening and reclamping of the Pacman cleft were ascertained from the temporal profiles of single-wavelength transient absorption signals. Figure 3 shows the traces for ΔOD of $(DPD)Fe_2O$ as a function of time for the transient absorption at 530 nm and the transient bleach at 565 nm. As mentioned above, the transient absorption signal for the "sprung open" state of the Pacman appears quickly, certainly within 20 ps of excitation for all four porphyrin systems. The rate constant for reclamping is given by $k_{reclamp}$

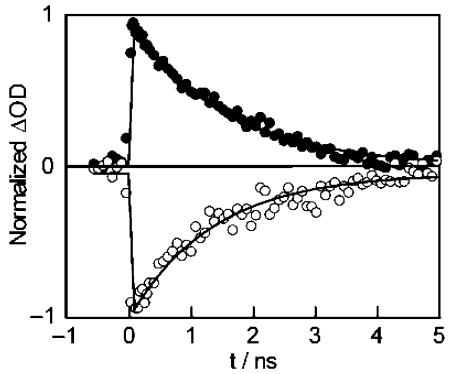

Figure 3. ΔOD as a function of time for $(DPD)Fe_2O$ following a 100-fs, 405-nm excitation pulse in the absence of a substrate. The probe wavelengths were 530 nm (solid) and 565 nm (open).

$= 1/\tau_o$, where τ_o is the lifetime of the transient intermediate. The decay kinetics are well-behaved, exhibiting monoexponential fits and wavelength independent time constants and completely returning to baseline. Table 1 lists the measured rate constants for the four systems of Chart 1. No signal is seen beyond 5 ns, confirming that irreversible photochemistry does not occur in the absence of substrate. Ground-state UV−visible spectra taken over the course of several hours of laser exposure show no change, consistent with control photolysis experiments in the absence of substrate.[30,34,37] Moreover, rate constants do not exhibit a power dependence, although the upper limit for this experiment was constrained to 2 μJ/pulse owing to the occurrence of thermal lensing at excess powers. This result establishes that the intramolecular opening and reclamping processes are triggered by the absorption of a single photon.

In the presence of sufficient concentration of substrate (S), the ferryl may be trapped before reclamping can occur. All porphyrins used in this study are thermally inert to $P(OMe)_3$; however, a clean and quantitative photolysis is obtained upon steady-state irradiation into the O−Fe LMCT transition at $\lambda_{exc} > 360$ nm in the presence of excess phosphite in benzene solution under anaerobic conditions. Electronic absorption and ^{31}P NMR analyses of the photoproducts establish the following transformation,[30]

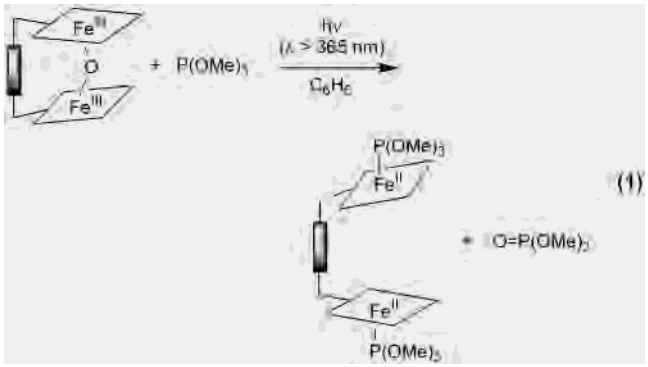

Table 1 lists photochemical quantum yields (Φ_p) for the photoreaction using $(DPD)Fe_2O$, $(DPX)Fe_2O$, $(DPXM)Fe_2O$, and $(Etio)_2Fe_2O$ as the photocatalyst. For these values of Φ_p, the concentration of the photoproduct (PFe^{II}/PFe^{II}) is too small to permit direct measurement of the rate constant for

(44) Shantha, P. K.; Verma, A. L. *Inorg. Chem.* **1996**, *35*, 2723−2725.
(45) Proniewicz, L. M.; Bajdor, K.; Nakamoto, K. *J. Phys. Chem.* **1986**, *90*, 1760−1766.
(46) Bajdor, K.; Nakamoto, K. *J. Am. Chem. Soc.* **1984**, *106*, 3045−3046.
(47) Rodgers, K. R.; Reed, R. A.; Su, Y. O.; Spiro, T. G. *Inorg. Chem.* **1992**, *31*, 2688−2700.
(48) Hashimoto, S.; Tatsuno, Y.; Kitagawa, T. *J. Am. Chem. Soc.* **1987**, *109*, 8096−8097.
(49) Hashimoto, S.; Mizutani, Y.; Tatsumo, Y.; Kitagawa, T. *J. Am. Chem. Soc.* **1991**, *113*, 6542−6549.
(50) Chin, D.-H.; La Mar, G. N.; Balch, A. L. *J. Am. Chem. Soc.* **1980**, *102*, 5945−5947.
(51) Miyake, H.; Chen, K.; Lange, S. J.; Que, J. L. *Inorg. Chem.* **2001**, *40*, 3534−3538.

Table 1. Lifetimes, $k_{reclamp}$, Φ_p, and Calculated k_{OAT} for the Series of Photosprung Diiron μ-Oxo Bisporphyrins in Benzene

			$P(OMe)_3$ oxidation	
compound	τ_o (ns)[a]	$k_{reclamp}$ (10^8 s^{-1})	k_{OAT} (M^{-1} s^{-1})[b]	Φ_p [c]
$(DPD)Fe_2O$	1.36(3)	7.4(2)	$1.1(1) \times 10^7$	$7.4(7) \times 10^{-4}$
$(DPX)Fe_2O$	1.26(5)	7.9(3)	$1.4(1) \times 10^3$	$9.0(1) \times 10^{-8}$
$(DPXM)Fe_2O$	1.27(9)	7.9(6)	$9(1) \times 10^4$	$5.5(6) \times 10^{-6}$
$(Etio)_2Fe_2O$	0.97(3)	10.3(4)	$1.3(1) \times 10^7$	$6.5(5) \times 10^{-4}$

[a] Averages of multiple measurements at λ_{det} = 460, 530, and 565 nm. [b] Values for k_{OAT} obtained using eq 2; Φ_{spring} is assumed to be 0.25 (see text). [c] Values of Φ_p for $(DPD)Fe_2O$ and $(DPX)Fe_2O$ taken from ref 30; values of Φ_p for $(DPXM)Fe_2O$ and $(Etio)_2Fe_2O$ measured according to the same procedure as in ref 30.

OAT (k_{OAT}) from the ferryl subunit to substrate; we estimate a $\Delta OD < 5 \times 10^{-5}$ for the highest quantum yield reaction and most positive assumptions for the photoreaction (see Supporting Information). Nevertheless, k_{OAT} may be ascertained indirectly by consideration of Φ_p in conjunction with the measured values of $k_{reclamp}$. Φ_p is the product of photocleavage (Φ_{spring}) and OAT quantum efficiencies, $\Phi_p = (\Phi_{spring}) \times (\Phi_{OAT})$. Expressing Φ_{OAT} in terms of the competing reclamping rate constant ($k_{reclamp}$) and the pseudo-first-order OAT rate constant ($k_{OAT}[S]$) leads to the following expression,

$$\Phi_p = \Phi_{spring} \frac{k_{OAT}[S]}{k_{OAT}[S] + k_{reclamp}} \qquad (2)$$

Table 1 gives the k_{OAT} values calculated using eq 2 for $P(OMe)_3$ oxidation. The lower limit for Φ_{spring} is estimated to be 0.25, based on the size of the initial transient signal measured (see Supporting Information); previous studies for the photocleavage of axial ligands from heme porphyrins have revealed near unit efficiency for this process.[38] Even if Φ_{spring} is underestimated, we believe it is constant across this series of compounds because the intensity of the transient signal is invariant for all systems under identical experimental conditions.

Discussion

The results of transient absorption and photochemistry for the series shown in Chart 1 are summarized by the catalytic cycle shown in Scheme 2. The primary photoproduct expected on LMCT excitation of a diiron(III) μ-oxo bisporphyrin, the $Fe_2^{II,III}$ oxyl radical, is not observed. Subsequent and rapid intramolecular electron transfer from the metal center to the oxyl radical causes iron−oxo bond photocleavage and production of the $PFe^{II}/PFe^{IV}O$ pair within 20 ps of the excitation pulse. The prevalence of $PFe^{IV}O$ versus $[PFe^{III}O]^-$ upon LMCT excitation is consistent with stereoelectronic requirements for subsequent reactivity according to the photocycle shown in Scheme 2. The tetragonal ligand field of the heme-oxo leads to the classic metal−ligand multiple bond d-orbital splitting diagram of a lowest energy singly degenerate $b_{2g}(d_{xy})$ orbital and an energetically proximate doubly degenerate $e_g(d_{xz},d_{yz})$ orbital set, which is able to establish an antibonding interaction with the oxygen p orbitals. For the case of the d^4 electron count of ferryl, the

Scheme 2

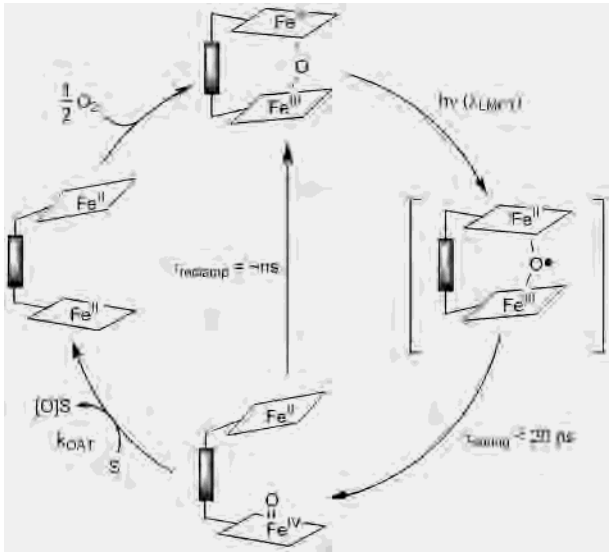

d_{xz} and d_{yz} orbitals of the e_g set are singly occupied, thus allowing for attack at the metal−oxo bond by nucleophilic substrates such as sulfides, phosphines, phosphites, and olefins. Conversely, this HOMO(substrate)−LUMO(heme-oxo) interaction is obviated by the d^6 electron count of the heme-oxide. The photocatalytic cycle is closed by the reaction of the diferrous form of the bisporphyrin with oxygen. Detailed studies by Balch and co-workers have uncovered the mechanism for the thermal formation of diiron(III) μ-oxo bisporphyrin complexes from unbridged iron(II) porphyrins in aerobic environments.[50,52−54] Unfortunately, we are not able to address this issue for Pacman photocatalysts in this study because the concentration of the diferrous form is too low to be directly observed by transient absorption spectroscopy. Thus, this aspect of the cycle will not be discussed further.

In the absence of substrate, the $PFe^{II}/PFe^{IV}O$ pair reclamps to form the $Fe^{III}-O-Fe^{III}$ core. The similarity of the $k_{reclamp}$ values in Table 1 establishes that the presence or nature of the bridge and peripheral substituents have little effect on the reclamping process. We find this to be a surprising result upon consideration of the X-ray structures for the $Fe^{III}-O-Fe^{III}$ Pacman porphyrins and their corresponding Zn^{II}_2 analogues, which provide a metric for a relaxed Pacman cleft. Owing to the presence of the six-membered heterocycle of the xanthene spacer, the metal−metal distances of the Zn^{II}_2 and $Fe^{III}-O-Fe^{III}$ DPX porphyrins are similar (d_{M-M} = 3.708 Å[30] and 3.50 Å,[55] respectively). The two porphyrin rings are cofacially presented with small lateral shift and in van der Waals contact. Thus, little distortion of the cofacial pocket of the DPX "bite" results upon photocleavage of the

(52) Latos-Grazynski, L.; Cheng, R.-J.; La Mar, G. N.; Balch, A. L. *J. Am. Chem. Soc.* **1982**, *104*, 5992−6000.
(53) Balch, A. L.; Chan, Y.-W.; Cheng, R.-J.; La Mar, G. N.; Latos-Grazynski, L.; Renner, M. W. *J. Am. Chem. Soc.* **1984**, *106*, 7779−7785.
(54) Balch, A. L. *Inorg. Chim. Acta* **1992**, *198*, 297−307.
(55) Chang, C. K. Department of Chemistry, Hong Kong University of Science and Technology, Clear Water Bay, Kowloon, Hong Kong, China. Personal communication, 2000.

$Fe^{III}-O-Fe^{III}$ bond. This is not the case for the DPXM and DPD porphyrins. A comparative structural analysis of $Zn(II)_2$ and $Fe^{III}-O-Fe^{III}$ DPD complexes shows that the clamped porphyrin is severely distorted; the metal−metal distance of the latter is compressed by more than 4 Å from the relaxed porphyrin pocket (d_{M-M} of $(DPD)Fe_2O = 3.504$ Å vs $d_{M-M} = 7.775$ Å for $Zn_2(DPD)$).[30] Photocleavage of the $Fe^{III}-O-Fe^{III}$ bond of the DPD platform therefore leads to significant relaxation of the porphyrin cleft. A similar situation exists for $(DPXM)Fe_2O$, though to a lesser extent. Steric clashing of the dimethoxyaryl substituents serves to pry open the cleft following $Fe^{III}-O-Fe^{III}$ photocleavage (d_{M-M} of $(DPXM)Fe_2O = 3.489$ Å vs d_{M-M} of relaxed $Zn_2(DPXM) = 5.913$ Å).[56,57] Correspondingly, the microscopic reverse of the spring reaction demands that tensely clamped porphyrin pockets re-form. Notwithstanding, the rates for $k_{reclamp}$ for the DPD, DPX, and DPXM systems are comparable. Even more surprising is the similarity of $k_{reclamp}$ for unbridged $(Etio)_2Fe_2O$ compared with the bridged counterparts. These data establish that reclamping is the predominant fate of a $PFe^{IV}O/PFe^{II}$ photocleaved pair even when the two porphyrin subunits are not covalently attached. This finding directly contradicts previous assumptions made in modeling $(TPP)_2Fe_2O$ photooxidation kinetics.[27] Our results for both tensely clamped Pacman porphyrins and unbridged bisporphyrins demonstrate the proclivity for $Fe^{III}-O-Fe^{III}$ bond formation in the oxidation photocatalysis of heme porphyrins.

When substrate is present in sufficient concentrations, the ferryl may be intercepted by an OAT reaction before reclamping can occur. As highlighted in Scheme 2, these two processes are in kinetic competition. Because $k_{reclamp}$ values for the three structurally disparate porphyrin systems are similar, the origin for any differences in photooxidation reactivity among the porphyrin systems must originate in the OAT step. Indeed, this is the case. Application of eq 2 reveals that k_{OAT} adheres to a trend consistent with the Pacman effect. For a given substrate, k_{OAT} is largest for the DPD cleft, rivaling that for the unbridged $(Etio)_2Fe_2O$ bisporphyrin. Presumably, the larger vertical span of the DPD pocket allows substrate easier side-on access to the iron−oxo bond. $(DPXM)Fe_2O$, with its intermediate vertical span, exhibits a k_{OAT} value that is intermediate between the DPX and DPD limits.

The results of the transient kinetics and X-ray crystallography studies are summarized in Figure 4. The origins of the Pacman effect are clearly evident. The value of k_{OAT} monotonically decreases as the vertical span of the relaxed cofacial cleft is decreased. These data are in striking contrast to the reclamping process, which shows no trend in the rate constant with the size of the cofacial cleft.

Extending the Pacman argument of Figure 4, $(Etio)_2Fe_2O$ porphyrin might be expected to display even higher photoactivity than $(DPD)Fe_2O$ Pacman porphyrin, in contrast to the observed results (see Table 1). The transient absorption studies of the two porphyrin systems resolve the apparent anomaly. For the unbridged system, the inability of the photocleaved PFe^{II} porphyrin to cage-escape from its $PFe^{IV}O$ partner suggests that a Pacman-like pocket is retained even when the two porphyrins are not cofacially attached. Presumably, the vertical span of the pocket for the caged porphyrins is similar to DPD, and hence, similar k_{OAT}'s are obtained.

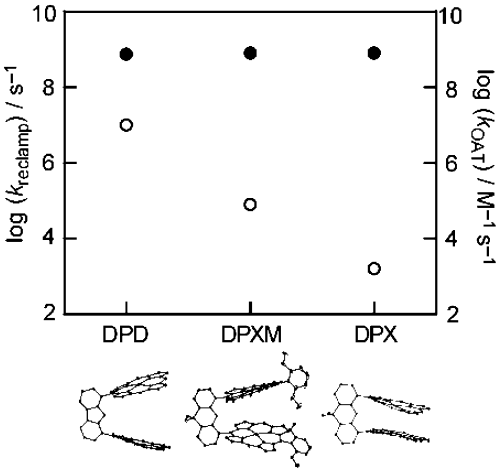

Figure 4. Values of $k_{reclamp}$ (●) and k_{OAT} (○) for cofacial bisporphyrins; k_{OAT} was calculated from eq 2 from the Φ_p for reaction 1. See text for cleft dimensions.

The Pacman effect, as manifested in substrate access to the iron−oxo bond, also accounts for the photooxidation efficiency of sterically demanding substrates. The photooxidation efficiency of the set of electronically homologous phosphite substrates increases along the series,[30]

phosphite:	$P(OMe)_3$ <	$P(OEt)_3$ ≪	$P(O\text{-}i\text{-}Pr)_3$ ≪	$P(OTMS)_3$
cone angle:	107	109	130	>172

As signified by the accompanying cone angles, the efficiency (and hence k_{OAT}) for photooxidation decreases with increasing steric bulk of the substrate. Moreover, the most sterically demanding phosphites such as $P(O\text{-}i\text{-}Pr)_3$ (*i*-Pr = isopropyl) and $P(OTMS)_3$ (TMS = trimethylsilyl) photoreact with $(DPD)Fe_2O$ but not with $(DPX)Fe_2O$. The superior photoreactivity (ca. 10 000-fold) of the diiron(III) μ-oxo DPD complex to oxidize phosphites is ascribed to the enhanced vertical range and flexibility that the dibenzofuran spacer provides for this cofacial platform.

Concluding Remarks

The multielectron oxidation photocatalysis of pillared cofacial diiron(III) μ-oxo bisporphyrins is governed by the vertical flexibility of the cofacial porphyrin, known as the Pacman effect. Transient absorption studies reveal that the diiron(III) μ-oxo DPD framework is structurally "spring-loaded" and cleavage of the Fe—O bond with a photon reveals the active ferryl species for the efficient side-on oxygen abstraction by substrate. Transient absorption studies show that the Pacman effect does not impede the reclamping of the ferryl to the neighboring ferrous porphyrin subunit. This result underscores the ability of the large thermodynamic

(56) Chang, C. J. Ph.D. Thesis, Massachusetts Institute of Technology, 2002.
(57) Chang, C. J.; Loh, Z.-H.; Rosenthal, J.; Shi, C.; Anson, F. C.; Nocera, D. G. Unpublished results.

driving force for diiron(III) μ-oxo formation to overcome kinetic impediments. Instead, the Pacman effect governs oxidation photocatalysis efficiencies by presenting a cofacial cleft of proper size and flexibility to efficiently accommodate substrate. Along these lines, our results establish that traditional cofacial bisporphyrins cannot be successfully exploited for OAT photocatalysis. The vertical span of (DPX)Fe_2O is only modestly more flexible than the two other cofacial porphyrins known previous to our studies, namely, cofacial porphyrins anchored to anthracene (DPA) and biphenylene (DPB).[58−71] The cofacial macrocycles for DPA, DPB, and DPX systems are in van der Waals contact and exhibit little vertical flexibility (ca. 1 Å) thus impeding substrate access to the terminal oxo. As demonstrated by the DPD platform, this limitation may be overcome when the cofacial platform is structurally "spring-loaded" to actively open and present a large cleft for the efficient side-on oxygen abstraction by substrate.

The photoreactivity of diiron bisporphyrins is of interest owing to their ability to utilize O_2 for oxidation reactions without the need for an external coreductant. The transient absorption study described here provides a road map to the design of more highly efficient systems. As seen from eq 2, because reclamping is in competition with the forward propagation of the photocycle, the efficiency for photocatalysis may be improved significantly if the escape yield of the $PFe^{II}/PFe^{IV}O$ pair can be increased (i.e., $k_{reclamp}$ decreased). Our results show that the cage escape yield is low, even for unbridged cofacial porphyrin subunits. Accordingly, new approaches to "spring-loaded" clefts should be explored. One attractive strategy involves the use of an electrostatic potential to drive the opening of the spring. Numerous studies of electron transfer have established that the cage escape yields increase dramatically for like-charged reactants.[72,73] The same principles should be applicable for like-charged $PFe^{II}/PFe^{IV}O$ subunits. These studies are currently underway.

Experimental Section

Materials. Free-base cofacial bisporphyrins H_2(DPD), H_2(DPX), and H_2(DPXM) were prepared as previously described.[30,31,33,74] The compounds gave satisfactory mass and ^{1}H NMR spectra. The untethered (Etio)$_2Fe_2O$ porphyrin was prepared from the free-base porphyrin, H_2(Etio), which was purchased from Sigma-Aldrich and used as received. The corresponding diiron μ-oxo compounds were prepared as previously described.[30,34]

Spectroscopy. Samples for spectroscopic measurements were contained within high-vacuum cells consisting of a 2 mm path length clear fused-quartz cell, which was connected to a 10 cm^3 solvent reservoir via a graded seal. The two chambers were isolated from the environment by a high-vacuum Teflon valve. Stock solutions of the diiron(III) μ-oxo bisporphyrins were added to the high-vacuum cell, and the solvent was removed on a high-vacuum manifold ($<10^{-6}$ Torr). The solvent reservoir was filled by vacuum transfer of spectroscopic grade benzene; the solution was subjected to three to five freeze−pump−thaw cycles under the high-vacuum manifold. The benzene was then transferred from the reservoir to the optical cell to yield a solution with a typical optical density of about 0.9 (ca. 5×10^{-5} M of the diiron(III) μ-oxo bisporphyrin) at the pump wavelength of 405 nm.

Picosecond transient absorption (TA) measurements were performed at 298 K on a chirped pulse amplified Ti:sapphire laser system. Sub-100-fs laser pulses were generated in a mode-locked Ti:sapphire oscillator (Coherent Mira 900), which is pumped by a 5-W continuous wave (CW) Coherent Verdi solid-state, frequency-doubled Nd:YVO_4 laser. The 76-MHz output was amplified in a regenerative amplifier cavity (BMI Alpha-1000) pumped by a 10-W Nd:YLF laser (BMI series 600) to generate a 1-kHz pulse train with central wavelength $\lambda_o = 810$ nm and a power of ~800 μJ/pulse. Pulse durations of 100 fs were measured with a Positive Light SSA single-shot autocorrelator. The output beam was split, with the majority component frequency doubled in a BBO crystal to produce 405-nm excitation pulses. The excitation power was typically attenuated to 2 μJ/pulse as higher powers resulted in thermal-lensing problems. Another 2 μJ/pulse of the 810-nm beam was focused into either a sapphire or a spinning CaF_2 substrate to generate a continuum probe pulse. Time resolution was achieved by propagating the excitation beam along a computer-controlled, 1.70-m long, optical delay line at 1 μm precision (Aerotech ATS 62150).

Transient absorption spectra were recorded at discrete times after excitation over the wavelength range of 390−630 nm. CaF_2 was the preferred substrate for continuum generation owing to a bluer achievable spectral limit ($\lambda = 370$ nm vs $\lambda = 470$ nm for sapphire).[75] The continuum spectrum of the probe light is shown in Supporting Information Figure 1. The probe pulse carries a chirp of roughly 2 ps, which was characterized by cross correlation of the pump and probe in a 5% solution of benzene in methanol. The polarizations of pump and probe pulses were set at the magic angle ($\theta_m = 54.7°$) and focused collinearly in the sample, which was stirred in the axis of beam propagation using a minimagnetic stir

(58) Collman, J. P.; Wagenknecht, P. S.; Hutchison, J. E. *Angew. Chem., Int. Ed. Engl.* **1994**, *33*, 1537−1554.
(59) Chang, C. K.; Abdalmuhdi, I. *J. Org. Chem.* **1983**, *48*, 5388−5390.
(60) Chang, C. K.; Abdalmuhdi, I. *Angew. Chem., Int. Ed. Engl.* **1984**, *23*, 164−165.
(61) Chang, C. K.; Liu, H. Y.; Abdalmuhdi, I. J. *J. Am. Chem. Soc.* **1984**, *106*, 2725−2726.
(62) Collman, J. P.; Hutchison, J. E.; Lopez, M. A.; Tabard, A.; Guilard, R.; Seok, W. K.; Ibers, J. A.; L'Her, M. *J. Am. Chem. Soc.* **1992**, *114*, 9869−9877.
(63) Collman, J. P.; Hutchinson, J. E.; Ennis, M. S.; Lopez, M. A.; Guilard, R. *J. Am. Chem. Soc.* **1992**, *114*, 8074−8080.
(64) Fillers, J. P.; Ravichandran, K. G.; Abdalmuhdi, I.; Tulinsky, A.; Chang, C. K. *J. Am. Chem. Soc.* **1986**, *108*, 417−424.
(65) Guilard, R.; Lopez, M. A.; Tabard, A.; Richard, P.; Lecomte, C.; Brandès, S.; Hutchison, J. E.; Collman, J. P. *J. Am. Chem. Soc.* **1992**, *114*, 9877−9889.
(66) Guilard, R.; Brandès, S.; Tardiex, C.; Tabard, A.; L'Her, M.; Miry, C.; Gouerec, P.; Knop, Y.; Collman, J. P. *J. Am. Chem. Soc.* **1995**, *117*, 11721−11729.
(67) Harvey, P. D.; Proulx, N.; Martin, G.; Drouin, M.; Nurco, D. J.; Smith, K. M.; Bolze, F.; Gros, C. P.; Guilard, R. *Inorg. Chem.* **2001**, *40*, 4134−4142.
(68) Le Mest, Y.; Inisan, C.; Laouenan, A.; L'Her, M.; Talarmain, J.; El Khalifa, M.; Saillard, J. Y. *J. Am. Chem. Soc.* **1997**, *119*, 6905−6106.
(69) Lui, H.-Y.; Abdalmuhdi, I.; Chang, C. K.; Anson, F. C. *J. Phys. Chem.* **1985**, *89*, 665−670.
(70) Ni, C.-L.; Abdalmuhdi, I.; Chang, C. K.; Anson, F. C. *J. Phys. Chem.* **1987**, *91*, 1158−1166.
(71) Naruta, Y.; Sasayama, M.; Ichihara, K. *J. Mol. Catal.* **1997**, *117*, 115−121.
(72) Newsham, M. D.; Cukier, R. I.; Nocera, D. G. *J. Phys. Chem.* **1991**, *95*, 9660−9666.
(73) Turro, C.; Zaleski, J. M.; Karabatsos, Y. M.; Nocera, D. G. *J. Am. Chem. Soc.* **1996**, *118*, 6060−6067.
(74) Chang, C. J.; Deng, Y.; Peng, S.-M.; Lee, G.-H.; Yeh, C.-Y.; Nocera, D. G. *Inorg. Chem.* **2002**, *41*, 3008−3016.
(75) Brodeur, A.; Chin, S. L. *J. Opt. Soc. Am. B* **1999**, *16*, 637−649.

bar. This procedure was implemented to prevent thermal lensing. In the spectral experiment, the probe beam exiting the sample was coupled into a liquid light guide to spatially homogenize the beam. The spectrum was then resolved in the monochromator (ISA Instruments, TRIAX 320) and recorded on a charge-coupled device (CCD) camera (Andor technology). The reference spectrum was taken at negative time. Typically, 3000 shots were accumulated per exposure and each time point was visited 30 times. Spectra taken from forward and reverse scans were averaged.

For single-wavelength kinetic measurements, sapphire was used for continuum generation owing to its superior stability. The cross correlation of the excitation beam with a single wavelength of the probe beam has a full width at half-maximum (fwhm) of 300 fs for the employed spectrometer configuration. The polarizations of the pump and probe beams were set at the magic angle relative to each other. The pump beam was mechanically chopped at 500 Hz and collinearly overlapped with the probe in the stirred sample. The probe beam was then spectrally resolved in the monochromator, a single wavelength selected, and the signal measured on a photodiode and amplified with a lock-in amplifier (Stanford Research Systems SR830), which was locked to the 500-Hz excitation frequency. Typically, the time range sampled was divided into 80 steps, including several steps at negative time. Ten forward and reverse scans were averaged.

The laser system used for nanosecond TA spectroscopy has been described elsewhere.[76] In this study, the third harmonic (355 nm) of the Nd:YAG was used as an excitation source. The 5-ns output pulses were delivered to sample at 20 Hz, with energies adjusted from 100 to 600 μJ/pulse. A 50-ns window of the intensified CCD camera was examined from 0 to 250 ns, and 1000 shots were averaged in each case. Transient spectra were collected on samples at 298 K over a wavelength range of 390−640 nm.

Photochemistry. Bulk photolyses were performed on stirred solutions contained in a quartz reaction vessel adapted for manipulations on a high-vacuum manifold. Samples were irradiated at 25 °C using a 1000-W high-pressure Oriel Hg−Xe lamp. The irradiation beam passed through cutoff filters to remove high-energy light and a collimating lens prior to entering the sample chamber. Quantum yield experiments were performed by replacing the cutoff filters with 10-nm band-pass mercury line interference filters (Oriel). The standard ferrioxalate technique was employed for the calculation of product quantum yields.[77] Photolysis reactions were monitored using absorption spectroscopy. Absorption spectra were obtained using a Cary-17 spectrophotometer modified by On-Line Instrument Systems (OLIS) to include computer control or a Spectral Instruments 440 model spectrophotometer.

Acknowledgment. We thank Dr. Niels H. Damrauer for significant contributions to the transient absorption experiment. C.J.C. thanks the National Science Foundation and the M.I.T./Merck Foundation for predoctoral fellowships. This work was supported by grants from the National Science Foundation (Grant CHE-0132680) and the National Institutes of Health (Grant GM 47274).

Supporting Information Available: Calculations of the maximum TA signal strength and lower limit of Φ_{spring} and the spectrum of the white light continuum produced from sapphire and CaF_2 substrates. This material is available free of charge via the Internet at http://pubs.acs.org.

IC034751O

(76) Loh, Z.-H.; Miller, S. E.; Chang, C. J.; Carpenter, S. D.; Nocera, D. G. *J. Phys. Chem. A* **2002**, *106*, 11700−11708.

(77) Murov, S. L.; Carmichael, I.; Hug, G. L. *Handbook of Photochemistry*, 2nd ed.; Marcel Dekker: New York, 1993.